BRIEF REPORTS

*Brief Reports are accounts of completed research which, while meeting the usual **Physical Review B** standards of scientific quality, do not warrant regular articles. A Brief Report may be no longer than four printed pages and must be accompanied by an abstract. The same publication schedule as for regular articles is followed, and page proofs are sent to authors.*

Energy dependence of quasiparticle damping at a metal surface

J. J. Deisz[*]

Department of Physics, Georgetown University, Washington, D.C. 20057

A. G. Eguiluz

Department of Physics and Astronomy, The University of Tennessee, Knoxville, Tennessee 37996-1200
and Solid State Division, Oak Ridge National Laboratory, Oak Ridge, Tennessee 37831-6032

(Received 7 May 1996)

We evaluate the energy dependence of the imaginary part of the electron self-energy ImΣ in the vicinity of a metal surface modeled with jellium via numerical calculations based on the GW approximation. When the electron is inside the surface, conventional quadratic scaling, Im$\Sigma \simeq (E-E_F)^2$ for $E \to E_F$, holds for electron positions all the way to the jellium edge and for energies at least up to the vacuum level $E-E_F \simeq 4$ eV. However, when the electron is in the vacuum outside the surface, large departures from quadratic scaling are obtained for most energies for which it holds in the bulk. These departures grow as the electron-surface separation increases. This effect is traced to the suppression of one-electron decay channels near the Fermi level. [S0163-1829(97)03915-5]

The dynamical properties of electrons in the vicinity of a metal surface are essential to a complete description of one- and two-photon photoemission spectroscopy, scanning tunneling microscopy, and electron-scattering experiments. A numerical scheme that treats the electrons as moving in an effective static one-body potential, such as that which appears in density-functional theory, often accounts for both occupied- and empty-state electron energy levels to a ''good'' degree of accuracy, i.e., errors are small on the electron volt scale that is typical of electronic bands. However, such a scheme does not reproduce an essential aspect of the corresponding quasiparticle excitations in a real, dynamically correlated system: a finite level width. These linewidths or quasiparticle damping rates must be accounted for via an explicit treatment of dynamical electronic correlations, usually through approximate evaluation of the imaginary part of the nonlocal, energy-dependent electron self-energy Im$\Sigma(\mathbf{x}_1,\mathbf{x}_2|\varepsilon)$, where $\varepsilon \equiv E - E_F$. Such calculations can then, perhaps, help characterize the essential many-body correlations that determine experimentally measurable linewidths.

A physical situation of relevance in this paper is the mea-

surement of image state linewidths by photoemission and inverse photoemission spectroscopy.[1–3] These linewidths probe the many-particle correlations in the vicinity of a metal surface,[4,5] to which electrons in these states are bound. While a parameter-free calculation of the electronic correlations for metal surfaces undoubtedly requires an accurate treatment of both the surface band structure and surface dynamics on a case-by-case basis, it is worthwhile to consider generic properties of electronic correlations that emerge as a result of the extremely anisotropic surface environment.

In this paper we report numerical results for the energy dependence of the imaginary part of the GW approximation for the electron self-energy in the vicinity of a metal surface modeled by jellium. We find that the energy dependence of ImΣ is dominated by conventional ε^2 scaling for $0.02\varepsilon_F < \varepsilon < 0.2\varepsilon_F$ ($\varepsilon_F = \hbar^2 k_F^2/2m_e$) for electron positions going from the jellium edge into the bulk. However, nonquadratic contributions to ImΣ become increasingly important, and eventually dominate, when the electron moves from the jellium edge into the vacuum—at least down to the lower end of the above range, for which accurate numerical results for ImΣ become increasingly difficult to obtain on account

of finite-size effects. We interpret this enhancement of non-quadratic contributions as a signature of a dual surface-induced process: (i) states near E_F are frozen out as possible final states on the vacuum side of the interface and (ii) higher-energy states have their probability amplitudes enhanced relative to their bulk counterparts.

We begin this discussion by noting the connection between the experimentally observable quasiparticle ($\varepsilon > 0$) linewidth Γ_{qp} and $\mathrm{Im}\Sigma$; this is given by

$$\Gamma_{qp} = 2 \int d\mathbf{x}_1 d\mathbf{x}_2 \psi_{qp}^*(\mathbf{x}_1) \mathrm{Im}\Sigma(\mathbf{x}_1,\mathbf{x}_2|\varepsilon_{qp}+i0^+)\psi_{qp}(\mathbf{x}_2). \tag{1}$$

Here we use the retarded self-energy, which is obtained by setting the frequency to just above the real axis in evaluating the Fourier transform of the time-ordered Σ; this imaginary frequency offset will henceforth be understood. For semiconductor Bloch states, numerical work has shown that the quasiparticle wave function in Eq. (1), $\psi_{qp}(\mathbf{x})$, is accurately obtained from density-functional theory calculations, even in the local-density approximation (LDA).[6,7] A similar conclusion has been reached for image states;[8] in that case the density-functional calculations must introduce long-range Coulomb correlations that are absent in the LDA.[9,10] Thus, at least for these cases, the dynamical correlations represented by Γ_{qp} are mainly contained in $\mathrm{Im}\Sigma$. In what follows, we focus our attention on the evaluation of $\mathrm{Im}\Sigma$ for coordinates near a metal surface, the vicinity to which being isolated by the image state quasiparticle wave functions entering Eq. (1).

A frequently employed approximation for the self-energy of weakly correlated metals and semiconductors is the GW or screened Hartree-Fock approximation,[11,12] given by

$$\Sigma(\mathbf{x}_1,\mathbf{x}_2|\varepsilon) = \frac{i}{2\pi} \int d\omega\, G(\mathbf{x}_1,\mathbf{x}_2|\varepsilon-\omega) W(\mathbf{x}_1,\mathbf{x}_2|\omega), \tag{2}$$

where $W(\mathbf{x}_1,\mathbf{x}_2|\omega)$ is the dynamically screened Coulomb interaction, with the screening evaluated in the random-phase approximation (RPA). Equation (2) and Dyson's equation provide a coupled set of equations that, in principle, should be satisfied self-consistently. However, it is common practice to perform a single iteration so that $G=G_0$ in Eq. (2), where G_0 is the electron Green's function obtained with electron-electron and electron-ion interactions represented by the static effective potential $v_{eff}=v_{ion}+v_{Hartree}+v_{xc}$, which arises in density-functional theory (DFT). For the jellium surface calculations considered here, the approximation $G\simeq G_0$ is supported by the near equivalence of the quasiparticle and DFT wave functions and energy levels for image states.[8]

After some algebra, the expression for the imaginary part of the retarded GW self-energy (for $\varepsilon > 0$ and with $G=G_0$) simplifies to

$$\mathrm{Im}\Sigma(\mathbf{x}_1,\mathbf{x}_2|\varepsilon) = \sum_{l \in \{l|0 < \varepsilon_l < \varepsilon\}} \psi_l^*(\mathbf{x}_1)\psi_l(\mathbf{x}_2)$$
$$\times \mathrm{Im}W(\mathbf{x}_1,\mathbf{x}_2|\varepsilon-\varepsilon_l), \tag{3}$$

where $\psi_l(\mathbf{x})$ and ε_l are DFT electronic wave functions and eigenvalues. Equation (3) has a simple interpretation. A quasiparticle with energy ε decays to an empty state of lower energy ε_l, with the excess energy $\varepsilon-\varepsilon_l$ transferred to either a plasmon or a particle-hole excitation. The dispersion relations of these excitations and their coupling to quasiparticles are given by $\mathrm{Im}W$. When ε is below the vacuum level, the decay into an empty state does not release enough energy ($\varepsilon_{vac}-\varepsilon_l \lesssim 4$ eV) to create a plasmon, except in low-density alkali metals where the plasma frequency is small. Thus, for the electron densities we have considered, Eq. (3) assigns the energy loss of a bound electron in vacuum to a particle-hole pair excitation that is created within a screening length of the surface.

To isolate the features of $\mathrm{Im}\Sigma(\mathbf{x}_1,\mathbf{x}_2|\varepsilon)$ that are independent of band-structure effects, we use the jellium model to represent the ions in a finite-width metal slab by a constant charge density $\rho_0 \equiv 3/4\pi r_s^3 a_B^3$ between two parallel "jellium edges" beyond which the effective ionic charge is zero. Electron wave functions and energies were obtained with an implementation of density-functional theory that self-consistently produces a $-1/4z$ surface potential barrier.[9,10] (We expect that the general features of the following results do not depend on the precise z dependence of the surface barrier.)

Numerical implementation of Eq. (3) for the jellium model requires the introduction of a set of systematic parameters. The jellium slab width turns out to have a strong impact on $\mathrm{Im}\Sigma$ for small ε; indeed, it proved necessary to consider slab widths of up to approximately $26\lambda_F$ to ensure that the "finite slab" effects are numerically insignificant while trying to approach the $\varepsilon \to 0$ limit. On this basis we believe our results are numerically accurate representations of a semi-infinite slab for ε values as small as $0.02\varepsilon_F$. $\mathrm{Im}\Sigma$ is evaluated in a mixed representation $\mathrm{Im}\Sigma(z_1,z_2|\mathbf{k}_\parallel,\varepsilon)$, where $\mathbf{k}_\parallel$ is the momentum of the quasiparticle in the spatially homogeneous x-y plane. Since we find that the $\mathbf{k}_\parallel$ dependence of $\mathrm{Im}\Sigma$ is extremely weak, $\mathbf{k}_\parallel$ is set equal to zero and does not play a role in the following results. After a Fourier transformation is applied to Eq. (3), an integral over final-state momenta parallel to the surface is required; this is approximated by a sum of up to 100 $\mathbf{q}_\parallel$ points. The z dependence of the screened interaction W is obtained by converting the RPA integral equation in $(\mathbf{q}_\parallel, z)$ space into a matrix equation whose rows and columns are labeled by discrete z points. A z spacing of $0.06\lambda_F$ is used to generate the results presented below; this produces convergence to within 1% at the absolute maximum and the absolute minimum of $\mathrm{Im}\Sigma$ and to within 3% at other relative maxima and minima. The infinitesimally small parameter $\delta \to 0^+$, which regulates the poles of $\mathrm{Im}W$ in Eq. (3), is varied from $0.01\varepsilon_F$ to $0.0001\varepsilon_F$ to broaden slightly δ functions that are not amenable to numerical calculations; this procedure represents the $\delta \to 0^+$ limit of $\mathrm{Im}\Sigma$ to well within 1%.

The top panel of Fig. 1 displays $v_{eff}(z)$ near the jellium edge ($z=0$) for $r_s = 1.5$, the electron-density parameter upon which we henceforth focus. For energies below the vacuum level (note that the vacuum level is approximately $0.2\varepsilon_F \simeq 4$ eV when the Fermi level is taken to be the zero of energy) but above E_F, $v_{eff}(z)$ will equal ε for some $z_{c,l} > 0$. This position corresponds to the classical turning point for a particle with $\mathbf{k}_\parallel = 0$. Quantum mechanics allows
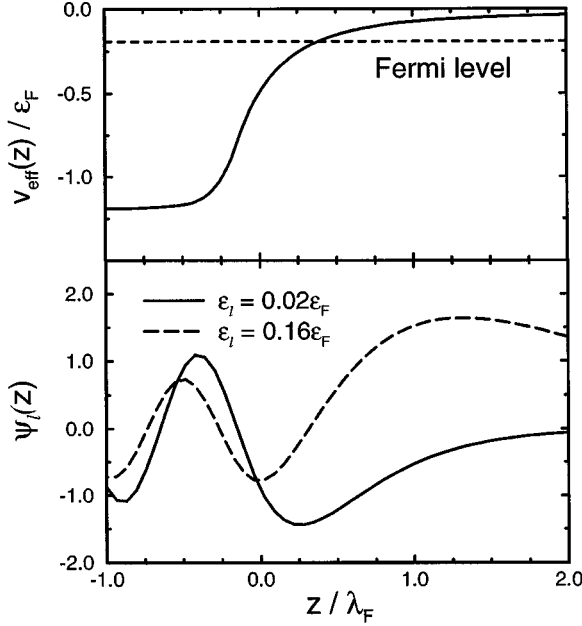
FIG. 1. Top: effective single-particle potential $v_{eff}(z)$ for a jellium model ($r_s \simeq 1.5$) of the surface, evaluated in the presence of long-range image effects [derived from the GW approximation Ref. 9]. Bottom: spatial dependence of typical final-state wave functions corresponding to quasiparticle decay in the image-state regime. The amplitude of the state near the vacuum level ($\varepsilon_l = 0.16\varepsilon_F$, where ε_l is given with respect to the Fermi level) is strongly enhanced on the vacuum side of the interface ($z > 0$) with respect to the state lying much closer to the Fermi level ($\varepsilon_l = 0.02\varepsilon_F$).
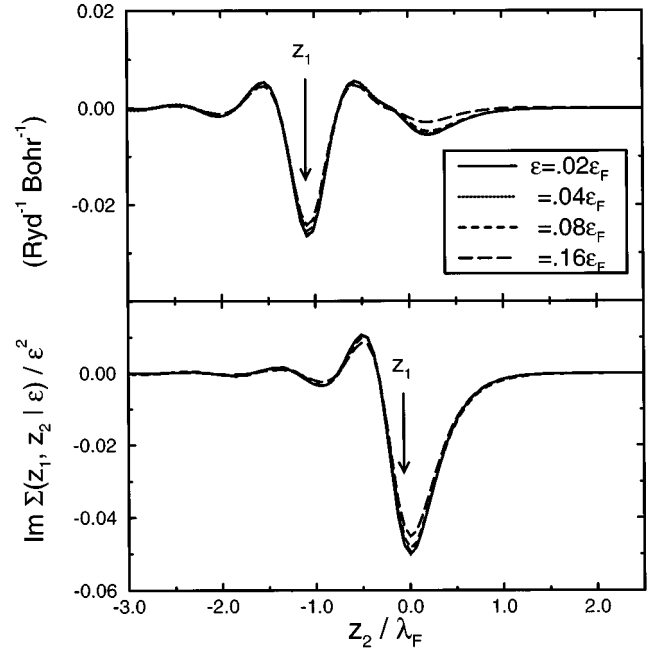

FIG. 2. Imaginary part of the self-energy $\text{Im}\Sigma(z_1, z_2 | \mathbf{k}_\parallel = \mathbf{0}, \varepsilon)$ divided by ε^2 for z_1 fixed one Fermi wavelength into the bulk (top) and z_1 fixed at the jellium edge (bottom), respectively. Although $\text{Im}\Sigma(z_1, z_2 | \mathbf{k}_\parallel = \mathbf{0}, \varepsilon)$ is sensitive to the presence of the surface, ε^2 scaling dominates for $0.02\varepsilon_F < \varepsilon < 0.16\varepsilon_F$.

states to tunnel into the vacuum beyond $z_{c,l}$, but the wave-function amplitude begins to decrease exponentially with distance from $z_{c,l}$. We illustrate this in the bottom panel of Fig. 1 with two wave functions, one corresponding to an energy just above the Fermi level ($\varepsilon_l = 0.02\varepsilon_F$) and the other to an energy just below the vacuum level ($\varepsilon_l = 0.16\varepsilon_F$). From this observation it follows that, as illustrated by the results presented below, the magnitude of $\text{Im}\Sigma$ begins to decrease quickly with increasing distance from the jellium edge as a result of the "freezing out" of final-state wave functions. It is less obvious that *the energy (and spatial) dependence of* $\text{Im}\Sigma$ should become *qualitatively* different from that for the bulk.

The behavior of $\text{Im}\Sigma(z_1, z_2 | \mathbf{k}_\parallel = \mathbf{0}, \varepsilon)/\varepsilon^2$ for electron coordinates going from the bulk to the jellium edge is displayed in Fig. 2. In the top panel, z_1 is fixed one Fermi wavelength ($\lambda_F \simeq 2.5\text{Å}$) inside the surface. As z_2 is scanned, the curves for different energies essentially lie on top of each other, except for $\varepsilon = 0.16\varepsilon_F$ where a small deviation becomes apparent near $z_2 = 0$. This result corresponds to the ε^2 scaling of quasiparticle damping in a bulk metal, a result that is expected to hold in the $\varepsilon \rightarrow 0$ limit on the basis of phase-space arguments[13] and has been borne out by specific application of the GW approximation to the bulk jellium model.[11] Note that our explicit numerical evaluation of $\text{Im}\Sigma$ shows that the domain of validity of quadratic scaling is much wider than analytic arguments[11] would suggest.

When z_1 is fixed at the jellium edge $z_1 = 0$, as shown in

the bottom panel of Fig. 2, we find that $\text{Im}\Sigma/\varepsilon^2$ is enhanced by about a factor of 2 relative to the bulk. There are no oscillations as z_2 goes into the vacuum as there are when z_2 is in the bulk. Despite these changes, ε^2 scaling still dominates over the entire energy range we have explored. Thus the extreme anisotropy of the surface itself does not lead to strong corrections to quadratic energy scaling for energies as high as the vacuum level.

Figure 3 displays $\text{Im}\Sigma/\varepsilon^2$ for z_1 fixed in the vacuum. The top panel corresponds to $z_1 \simeq 0.5\lambda_F$; in this case the magnitude of $\text{Im}\Sigma$ is roughly equivalent to that for the jellium edge, as seen in Fig. 2. However, it is evident that scaling $\text{Im}\Sigma$ by $1/\varepsilon^2$ does not produce the overlap between the various curves for $0.02\varepsilon_F \leq \varepsilon \leq 0.16\varepsilon_F$, which was observed when the electron was either in the bulk or at the jellium edge. This result signals a dramatic enhancement of corrections to quadratic scaling, an effect that appears concomitantly with the extreme nonlocality of $\text{Im}\Sigma$.[8,14] (By extreme nonlocality we mean the following: the maximum magnitude of $\text{Im}\Sigma$ occurs at $z_2 \simeq 0$ rather than for $z_2 \simeq z_1$.)

The overall magnitude of $\text{Im}\Sigma/\varepsilon^2$ decreases as z_1 is increased to λ_F, as seen in the bottom panel of Fig. 3. At the same time, there is a large increase in the relative size of corrections to quadratic scaling. Clearly, the nonquadratic contributions dominate the result for $\varepsilon = 0.16\varepsilon_F$. Nonetheless, our results suggest that the scaled curves for $\text{Im}\Sigma$ approaches a unique, nonzero limit as $\varepsilon \rightarrow 0$, i.e., curves computed strictly in this limit will overlap. This suggests that quadratic scaling will eventually hold at a sufficiently low energy.[13]
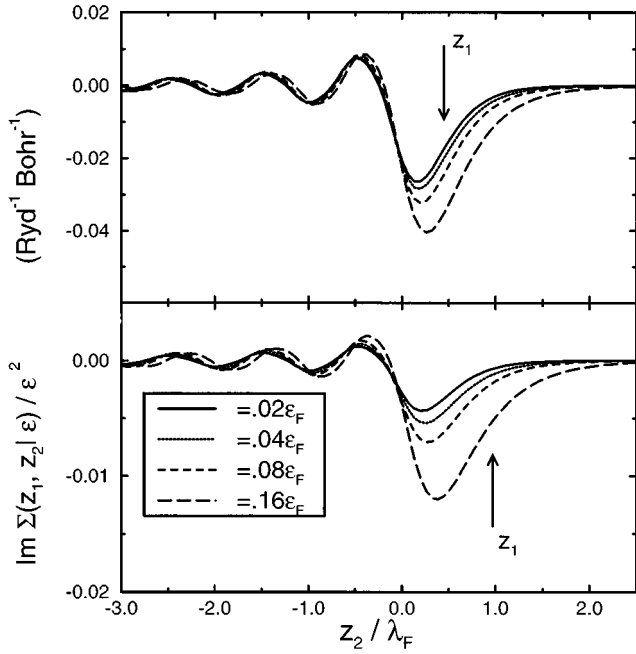
FIG. 3. Scaled imaginary part of the self-energy $\mathrm{Im}\Sigma(z_1,z_2|\mathbf{k}_\parallel=\mathbf{0},\varepsilon)/\varepsilon^2$ for z_1 one-half (top) and one (bottom) Fermi wavelength into the vacuum. Large corrections to quadratic energy scaling are observed; they become increasingly dominant as z_1 moves from the surface into the vacuum.

(A comparison of the results for $z_1 \simeq 0.5\lambda_F$ and $z_1 \simeq \lambda_F$ suggests that the energy range where quadratic scaling dominates becomes progressively smaller as z_1 goes further into the vacuum. Unfortunately, the small magnitude of the vacuum self-energy as well as the slowly converging finite-slab effects for small ε prevent us from making a more quantitative study of the $\varepsilon \to 0$ regime.)

To discuss these features of $\mathrm{Im}\Sigma$ in vacuum, we return to Eq. (3). Quasiparticle decays at the jellium edge and in the vacuum are both accompanied by particle-hole excitations near the jellium edge. This suggests that it is the set of final-state wave functions $\{\psi_l(\mathbf{x})\}$, and not $\mathrm{Im}W$, that is responsible for the unusual behavior of $\mathrm{Im}\Sigma$ in vacuum. As shown in the bottom panel of Fig. 1, the final-state wave functions have exponentially reduced amplitudes beyond $z_{c,l}$. This leads to a surface-induced spatial and energy dependence of the wave functions, approximately given by

$$\psi_l(z) \simeq \exp\left(-\int_{z_{c,l}}^{z}\sqrt{2m[v_{\mathrm{eff}}(z)-\varepsilon_l-\hbar^2 k_\parallel^2/2m]/\hbar^2}\,dz\right),$$

$$z > z_{c,l}, \quad (4)$$

which must supplement the traditional phase-space arguments that yield quadratic scaling when the final-state wave functions are plane waves.[13]

The extreme nonlocality of $\mathrm{Im}\Sigma$ may also be understood from the tunneling form of the final-state wave functions in vacuum. For $\mathbf{x}_1$ fixed in the vacuum, $\mathcal{O}_l(\mathbf{x}_1,\mathbf{x}_2) \equiv |\psi_l^*(\mathbf{x}_1)\psi_l(\mathbf{x}_2)|$ grows as $\mathbf{x}_2$ moves away from $\mathbf{x}_1$ and towards the surface. The maximum value of $\mathcal{O}_l(\mathbf{x}_1,\mathbf{x}_2)$ occurs near $z_2 = z_{c,l}$, after which $\mathcal{O}_l(\mathbf{x}_1,\mathbf{x}_2)$ oscillates as $\mathbf{x}_2$ enters the bulk. However, as $\mathbf{x}_2$ enters the bulk, the screening described by $\mathrm{Im}W$ begins to reduce the magnitude of the $\psi_l(\mathbf{x})$'s contribution to $\mathrm{Im}\Sigma$ in Eq. (3).

In conclusion, we have demonstrated a unique aspect of many-body correlations for a strongly inhomogeneous electronic system: a metal surface modeled by jellium. For a quasiparticle in the vacuum outside the surface, large corrections to quadratic energy scaling have been obtained on the basis of a numerical implementation of the GW approximation that includes a self-consistent treatment of surface inhomogeneity. These corrections are due to final-state wave functions changing from propagating states in the bulk to tunneling states in the vacuum. Of course, one may wonder if the physics discussed in this paper may lead to observable effects. This issue will be addressed in a future work,[15] in which we plan to determine the relative importance of the vacuum self-energy, and the associated departure from quadratic energy scaling, in a quantitative evaluation of the linewidth for a specific physical system, namely the image states of Pd(111).

[*]Present address: 930 NW 25th Place #210, Portland, OR 97210.

[1]N. Fischer, S. Schuppler, Th. Fauster, and W. Steinmann, Phys. Rev. B **42**, 9717 (1990).

[2]S. Schuppler, N. Fischer, Th. Fauster, and W. Steinmann, Phys. Rev. Lett. **46**, 13 539 (1992).

[3]R. Fischer, S. Schuppler, N. Fischer, Th. Fauster, and W. Steinmann, Phys. Rev. Lett. **70**, 654 (1993).

[4]P.M. Echenique, F. Flores, and F. Sols, Phys. Rev. Lett. **55**, 2348 (1985); P.M. Echenique, J. Phys. C **18**, L1133 (1985); P. de Andrés, P.M. Echenique, and F. Flores, Phys. Rev. B **35**, 4529 (1987); P.L. de Andres, P.M. Echenique, and F. Flores, *ibid.* **39**, 10 356 (1989).

[5]S. Gao and B.I. Lundqvist, Prog. Theor. Phys. Suppl. **106**, 405 (1991).

[6]M.S. Hybertsen and S.G. Louie, Phys. Rev. Lett. **55**, 1418 (1985).

[7]M.S. Hybertsen and S.G. Louie, Phys. Rev. B **38**, 4033 (1988).

[8]J.J. Deisz, A.G. Eguiluz, and W. Hanke, Phys. Rev. Lett. **71**, 2793 (1993).

[9]A.G. Eguiluz, M. Heinrichsmeier, A. Fleszar, and W. Hanke, Phys. Rev. Lett. **68**, 1359 (1992).

[10]A.G. Eguiluz, J.J. Deisz, M. Heinrichsmeier, A. Fleszar, and W. Hanke, Int. J. Quantum Chem. Quantum Chem. Symp. **26**, 837 (1992).

[11]J.J. Quinn and R.A. Ferrel, Phys. Rev. **112**, 812 (1958).

[12] L. Hedin and S. Lundqvist, in *Solid State Physics*, edited by H. Ehrenreich, F. Seitz, and D. Turnbull (Academic, New York, 1969), Vol. 23, p. 1.

[13] See, for example, J.W. Negele and H. Orland, *Quantum Many-Particle Systems* (Addison-Wesley, Redwood City, CA, 1988), p. 254.

[14] J. Deisz and A.G. Eguiluz, J. Phys.: Condens. Matter **5**, A95 (1993).

[15] J.J. Deisz, A. Fleszar, M. Heinrichsmeier, and A.G. Eguiluz (unpublished).